**RMetS**

Royal Meteorological Society

# Different long-term trends of extra-tropical cyclones and windstorms in ERA-20C and NOAA-20CR reanalyses

Daniel J. Befort,[1,]* Simon Wild,[1] Tim Kruschke,[2] Uwe Ulbrich[3] and Gregor C. Leckebusch[1]

[1]*School of Geography, Earth and Environmental Sciences, University of Birmingham, UK*
[2]*Department of Ocean Circulation and Climate Dynamics Research Unit Marine Meteorology, GEOMAR Helmholtz Centre for Ocean Research Kiel, Germany*
[3]*Institute of Meteorology, Freie Universität Berlin, Germany*

*Correspondence to:
D. J. Befort, School of Geography, Earth and Environmental Sciences, University of Birmingham, B15 2TT Birmingham, UK.
E-mail: d.j.befort@bham.ac.uk*

## Abstract

NOAA 20th century and ERA-20C reanalysis datasets are evaluated regarding the representation of extra-tropical cyclones and windstorms over the Northern and Southern Hemisphere during the respective 6-month winter seasons. The results indicate substantial differences in low-frequency variability between the two datasets – especially in the first half of the 20th century – expressed in different signs and/or magnitudes of long-term trends. This is hampering a reliable analysis of real long-term trends of cyclone and windstorm activity. However, higher-frequency variability is in good agreement between both datasets especially for the Northern Hemisphere.

**Keywords:** extra-tropical cyclones; windstorm events; reanalysis data

## 1. Introduction

Windstorms caused by extra-tropical cyclones are one of the major natural hazards in the mid-latitudes of both hemispheres. They can kill people, disrupt critical infrastructure, damage buildings and industry installations and generate large economic losses. One example of a particularly stormy winter was 2013/2014 over the UK (cf. Kendon and McCarthy, 2015), which was classed as the most active season regarding windstorm frequency for at least the last 35 years (Wild *et al.*, 2015) and the most active season regarding cyclone frequency for over a century in the UK (Matthews *et al.*, 2014). For the Southern Hemisphere land extent is less in the latitudes of interest, meaning less direct impacts on losses, though severe windstorms are generally an even more pronounced feature over the ocean here than in the Northern Hemisphere (hence the terms 'roaring forties' and 'furious fifties'). These can have severe consequences for shipping in the southern ocean (e.g. Lim and Simmonds, 2002; Revell, 2015).

While our understanding of synoptic scale processes involved in the generation of (severe) extra-tropical cyclones is generally well developed, scientific research has not fully understood the governing physical processes steering the variability of storm frequencies on time scales from inter-annual to multi-decadal (see for inter-annual variability, e.g. Wild *et al.* 2015; Huntingford *et al.*, 2014). For Europe, the influence of ocean heat content anomalies over the North Atlantic has recently been highlighted by Nissen *et al.* (2014a), using coupled climate model simulations. As climate model responses to such anomalies are often model specific (e.g. Yu and Weller, 2007), it is important to assess

observed variability. Physically consistent, global gridded three-dimensional datasets for the past have been produced by different re-analysis projects. The NOAA-20CR dataset (Compo *et al.*, 2011) was used by Donat *et al.* (2011), suggesting long-term trends in extreme storms in the NOAA-20CR ensemble for the European region. This finding triggered a scientific discussion about the reliability of historic trends derived from reanalyses and estimates from station observations in specific regions (e.g. Brönnimann *et al.*, 2012; Krueger *et al.*, 2013, 2014; Wang *et al.*, 2013, 2014). With the release of the ECMWF 20th century reanalysis (ERA-20C; Poli *et al.*, 2013) a new data set is now available to investigate the multi-decadal variability of extreme mid-latitude cyclone and windstorm events. In addition to mean-sea level pressure (MSLP) observations (as used by NOAA-20CR), surface wind observations over the oceans are also assimilated. Our present study compares trends in these two reanalysis datasets, considering both extra-tropical cyclones and strong, potentially damaging wind events over both hemispheres. We address the question of different trends in the two datasets, their time dependency and separate between multi-decadal and high-frequency spectral components.

## 2. Data and methods

In this study the ECMWF 20th century reanalysis (ERA-20C) dataset with a horizontal resolution of T159 (1.125°) and 91 vertical levels for the period 1901 until 2008 is used. Atmospheric pressure observations as well as near-surface wind observations over the

oceans are assimilated employing a 4D-Var-scheme (Poli *et al.*, 2013). Sea-surface temperature and sea ice conditions are provided by the HadISST2.1.0.0 (Titchner and Rayner, 2014) dataset. Additionally, the NOAA 20th century reanalysis datasets (NOAA-20CR (v2), Compo *et al.*, 2011) with a horizontal resolution of 2° for the period from 1871 until 2009 is analysed. In this case, sea-surface temperature and sea ice conditions are taken from the HadISST1.1 dataset (Rayner *et al.*, 2003), whereas only atmospheric pressure observations are assimilated, employing an Ensemble Kalman Filter, producing a reanalysis ensemble with 56 members.

Cyclones are identified in the Northern and Southern Hemisphere extra-tropics (excluding the tropical belt within 20°N–20°S). Cyclones are identified and tracked using the algorithm developed by Murray and Simmonds (1991). This algorithm has been used by several studies investigating extra-tropical cyclones under recent and future climate conditions (Leckebusch and Ulbrich, 2004; Pinto *et al.*, 2005; Leckebusch *et al.*, 2006; Kruschke *et al.*, 2014) and is included in the intercomparison of mid-latitude storm diagnostics initiative (Ulbrich *et al.*, 2013; Neu *et al.*, 2013). Six hourly MSLP fields are used as input, which are available for both datasets: ERA-20C and NOAA-20CR. Analyses are carried out for all cyclones and for the most extreme events. Extreme cyclones are defined as those events with a minimum core pressure below 970 hPa over the Northern and below 960 hPa over the Southern Hemisphere, in accordance with Lambert and Fyfe (2006).

The representation of extreme windstorms in reanalysis products is not perfect. Like model simulations of comparable resolution they underestimate maximum gusts in terms of absolute measures (e.g. Hewson and Neu, 2015). For this reason an algorithm introduced by Leckebusch *et al.* (2008) which identifies windstorms based on instantaneous near-surface wind speeds relative to the climatology of the respective dataset is applied. The method identifies areas in which wind speeds exceed the local 98th percentile. A minimum affected area of $150\,000\,km^2$ is required for assigning the 'windstorm' attribute to a weather situation. Tracking of windstorm fields is primarily based on a nearest-neighbour approach. Windstorm tracks lasting less than 18 hours are excluded from the statistics. A comprehensive description of the scheme is given by Kruschke (2015). This algorithm has been proven useful in several studies to identify extra-tropical windstorm events in gridded climate data (e.g. Renggli *et al.*, 2011, Nissen *et al.*, 2014a, 2014b, Befort *et al.*, 2015, Kruschke *et al.*, 2015, Wild *et al.*, 2015). In general, these studies used 10-m level wind speeds for their analyses. This parameter is only available for ERA-20C, but not for NOAA-20CR. Therefore the 0.995 sigma level (~1008 hPa/44 m using a surface pressure of 1013 hPa) for NOAA-20CR is used instead. Sensitivity tests using ERA-20C confirmed that this difference in base height yields no large impact on the temporal variability of windstorms nor the absolute number of events identified. The 98th percentile of each dataset (NOAA-20CR, ERA-20C) is calculated for the years from 1961 until 2000.

Windstorm as well as cyclone events are identified over both hemispheres for the extended winter season (NH: October to March; SH: April to September). In case of NOAA-20CR, events are identified for all 56 ensemble member separately. Spatial track densities are calculated similar to Kruschke *et al.* (2014), but using a 'search' radius of 700 km. To analyse in how far differences between both datasets change in time, analyses are carried out for the periods 1901–1930, 1931–1960 and 1961–1990. Additionally, the number of cyclones/windstorms within three northern hemispheric regions (Northern Europe, North Atlantic, Polar Region, see Figure 1(a)) and three southern hemispheric regions (Atlantic Ocean, Indian Ocean, Pacific Ocean, see Figure 4(a)) is analysed. A Lanczos low-pass filter (Duchon, 1979) with a cut-off frequency of $1/31\,years^{-1}$ using 31 weights is applied to investigate the lower-frequency variability. The high-pass filtered time series are obtained by calculating the residuum between the original and the low-pass filtered time series. Eventually, a linear regression model is fitted to the original time series (the ensemble mean for NOAA-20CR) for each period. The similarity of low-frequency variability (LFV) between both datasets is assessed by calculating the difference of the relative linear regression slope for each period using a common reference period (1961–1990). A Mann–Kendall test is applied to test the significance of the long-term trends. The similarity of the high-frequency variability (HFV) is assessed by correlation coefficients between both high-pass filtered time series, which is only possible for the second and third period as no low-pass filtered information is available for the complete first period.

## 3. Results

### 3.1. Northern Hemisphere (NH)

#### 3.1.1. All cyclone events

The cyclone track density pattern (Figure 1(a), for the 1961–1990 period) is characterized by the two well-known centres of activity over the North Atlantic and North Pacific. It is assumed that the quality of both reanalyses is best for this most recent period. Consequently, the highest agreement between both datasets is expected for the last period. However, more cyclone tracks for ERA-20C than in NOAA-20CR are found (about 29% between 1961 and 1990 over the Northern Hemisphere using ERA-20C as reference), which is partly related to the finer resolution of ERA-20C (see Pinto *et al.*, 2005). Consistently, about 11% fewer cyclones over the Northern Hemisphere are identified when interpolating the ERA-20C data to the coarser NOAA-20CR grid compared to the original ERA-20C data. Note that interpolating to a coarser resolution will not lead to the same results as running the model on a coarser resolution, because
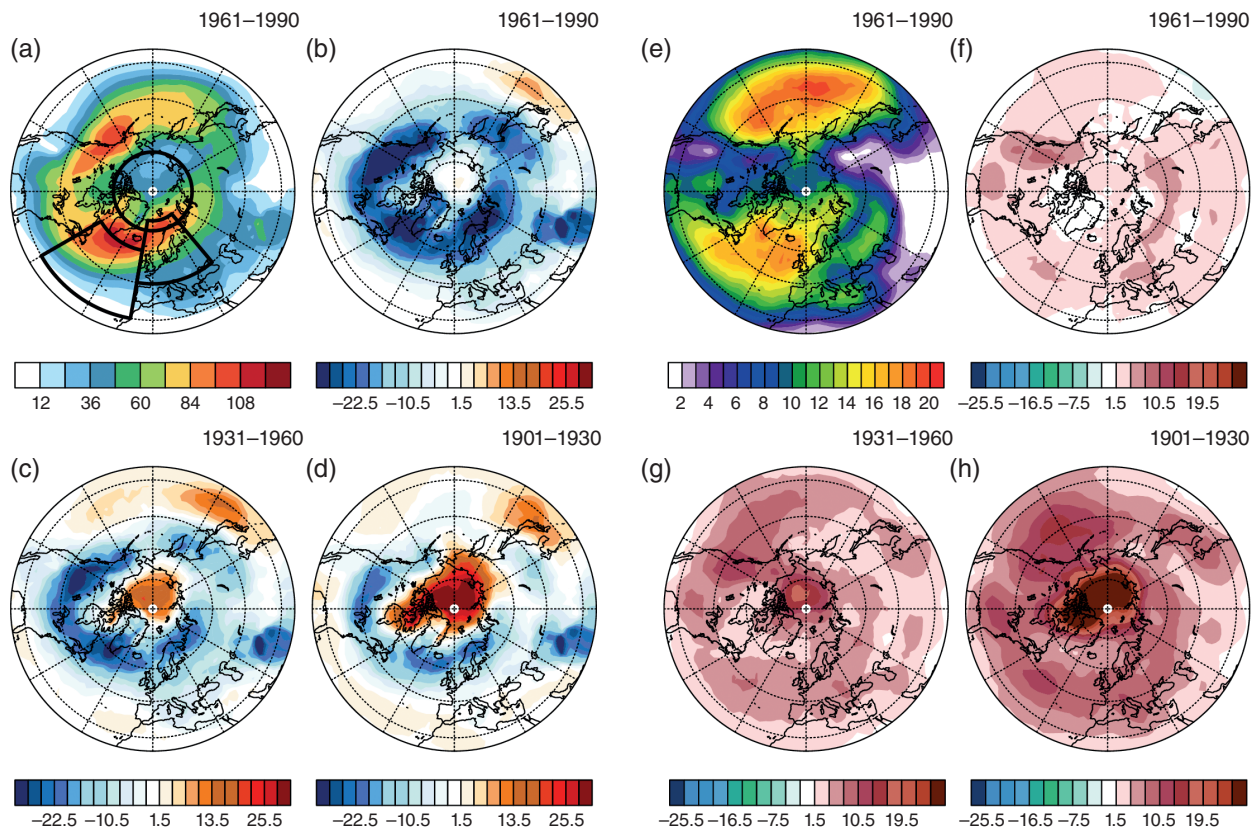
**Figure 1.** Track densities for cyclones (a–d) and windstorms (e–h) over the Northern Hemisphere in number of events per season. Cyclones: (a) ERA-20C (1961–1990), (b) NOAA-20CR minus ERA-20C (1961–1990), (c) NOAA-20CR minus ERA-20C (1931–1960) and (d) NOAA-20CR minus ERA-20C (1901–1930). Windstorms: (e) ERA-20C (1961–1990), (f) NOAA-20CR minus ERA-20C (1961–1990), (g) NOAA-20CR minus ERA-20C (1931–1960) and (h) NOAA-20CR minus ERA-20C (1901–1930). Northern Hemispheric regions used for time series analyses (North Atlantic, Northern Europe, Polar Region) are shown (a).

more processes are resolved in simulations with higher resolution.

Trends of cyclone track numbers over the NH differ drastically between the two datasets for the first (1901–1930) and second (1931–1960) period (Figure 2(a)). For the first period an increasing trend of cyclones is found for both datasets, which is smaller in ERA-20C compared to those in NOAA-20CR. For the second period the long-term trend reverses in NOAA-20CR, yet the increasing trend is still found for ERA-20C. The disagreement in the first and second period is due to a distinct increase of events over the Polar Region and (to a lower degree) over the North Atlantic with its maximum around the year 1920 in the NOAA-20CR dataset, which is not present in the ERA-20C (Figure 2(a), (c) and (d)). The NOAA-20CR maximum is followed by a decreasing trend until the end of the century, again mainly influenced by the Polar Region, while ERA-20C shows a positive trend from 1900 until 1960 both over the entire hemisphere and over the pole. A good agreement between ERA-20C and NOAA-20CR is found for the last period.

Long-term trends between ERA-20C and NOAA-20CR differ in their sign and magnitude for most selected northern hemispheric regions for the first and second period, while a better agreement is found during the third period. It should be noted that even

though the sign of the linear trends differ partly, the individual trends in each dataset are often not significant.

Assessing similarity of the HFV, generally positive correlations are found for all periods and regions, with highest coefficients (above 0.7) for the third period.
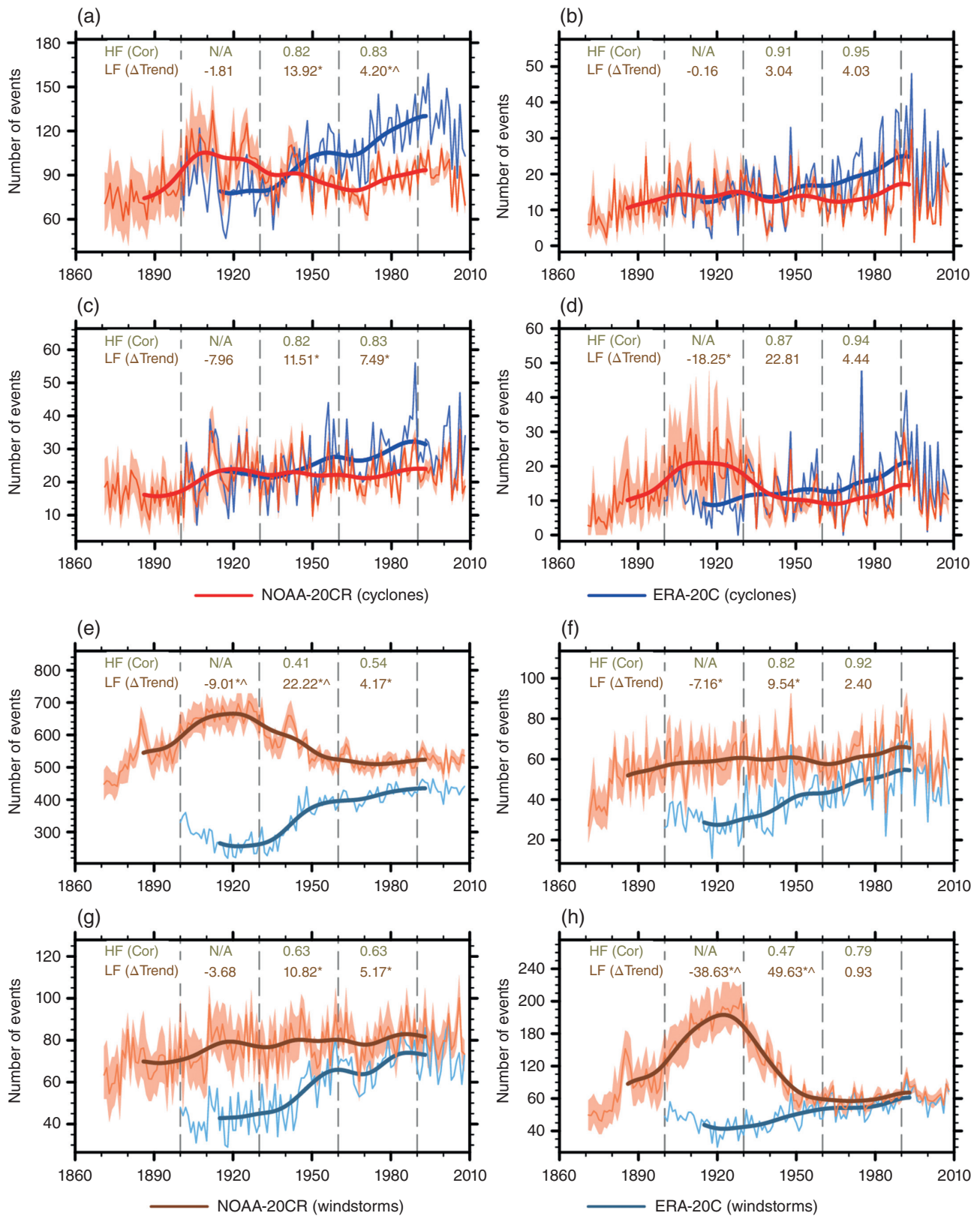
### 3.1.2. *Extreme cyclone events*

The analysis of the extreme cyclones (core pressure below 970 hPa) shows a reduced maximum of cyclone events around 1920 in NOAA-20CR (Figure 3(a)) compared to all cyclones (Figure 2(a)). This suggests that the increased number of all cyclone events around 1920 is mainly due to weaker events. An increased number of events around 1990 is found in both datasets and in all regions. In general, LFV of extreme cyclones is in better agreement between ERA-20C and NOAA-20CR compared to all cyclones. Long-term trends show the same sign in all regions and all periods except for the second period over the Northern Hemisphere (Figure 3(a)–(d)). However, only ERA-20C shows a trend significantly different from zero for the second period over the Northern Hemisphere (Figure 3(a)). Despite the same sign of trends for most periods and regions, large differences in their magnitudes are found, e.g. of about 4% per decade during the third period over Northern Europe (Figure 3(b)).
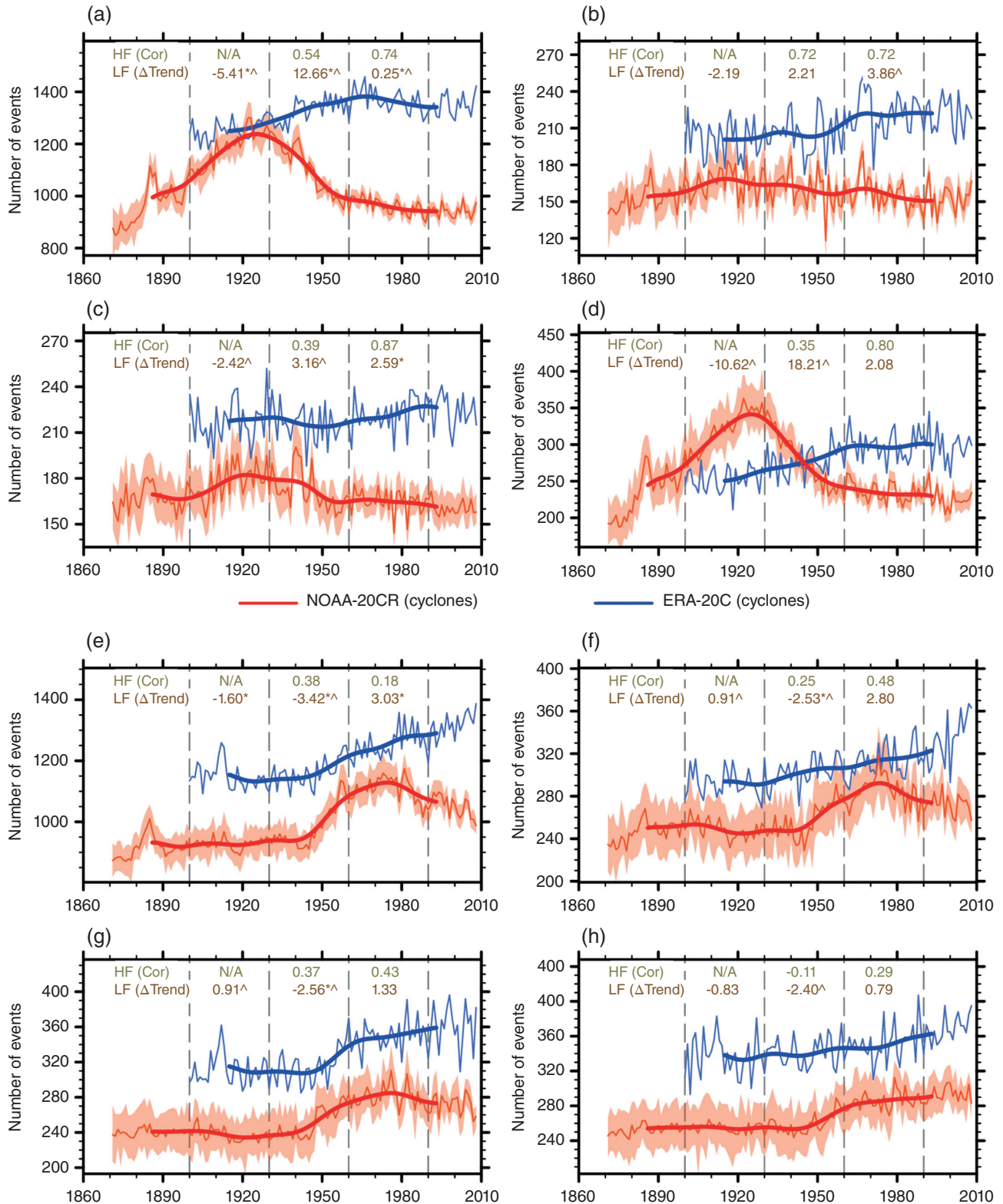
**Figure 2.** Time series of cyclone events for three selected regions over the Northern Hemisphere (a–d) and Southern Hemisphere (e–h). Northern Hemisphere: (a) extra-tropical NH, (b) Northern Europe, (c) North Atlantic and (d) Polar Region (see Figure 1(a) for NH regions). Southern Hemisphere: (e) extra-tropical SH, (f) Atlantic Ocean, (g) Indian Ocean and (h) Pacific Ocean. (see Figure 4(a) for SH regions). The bold lines indicate the low-pass filtered time series (with a cut-off frequency of 1 per 31 years). NOAA-20CR ensemble mean is shown as the red thin line, whereas the ensemble spread is indicated as shaded area. The similarity of the high frequency (HF) is given as correlation coefficients (green values, top of each Figure). Relative differences (ERA-20C−NOAA-20CR) of linear regression coefficients are given in % events per decade using a common reference period from 1961 to 1990. The coefficients are bold if trends differ in sign. Superscripts* and ^ indicate trends significantly different from zero (ERA-20C (*) and/or NOAA- 20CR(^)).

**Figure 3.** Time series of extreme cyclone events (minimum core pressure below 970 hPa) (a–d) and windstorm events (e–h) for three selected regions over the Northern Hemisphere. Cyclones: (a) extra-tropical NH, (b) Northern Europe, (c) North Atlantic and d) Polar Region (see Figure 1 for NH regions). Windstorms: (e) extra-tropical NH, (f) Northern Europe, (g) North Atlantic and (h) Polar Region (see Figure 1 for NH regions). Time series, correlations and trend characteristics analogue to Figure 2.
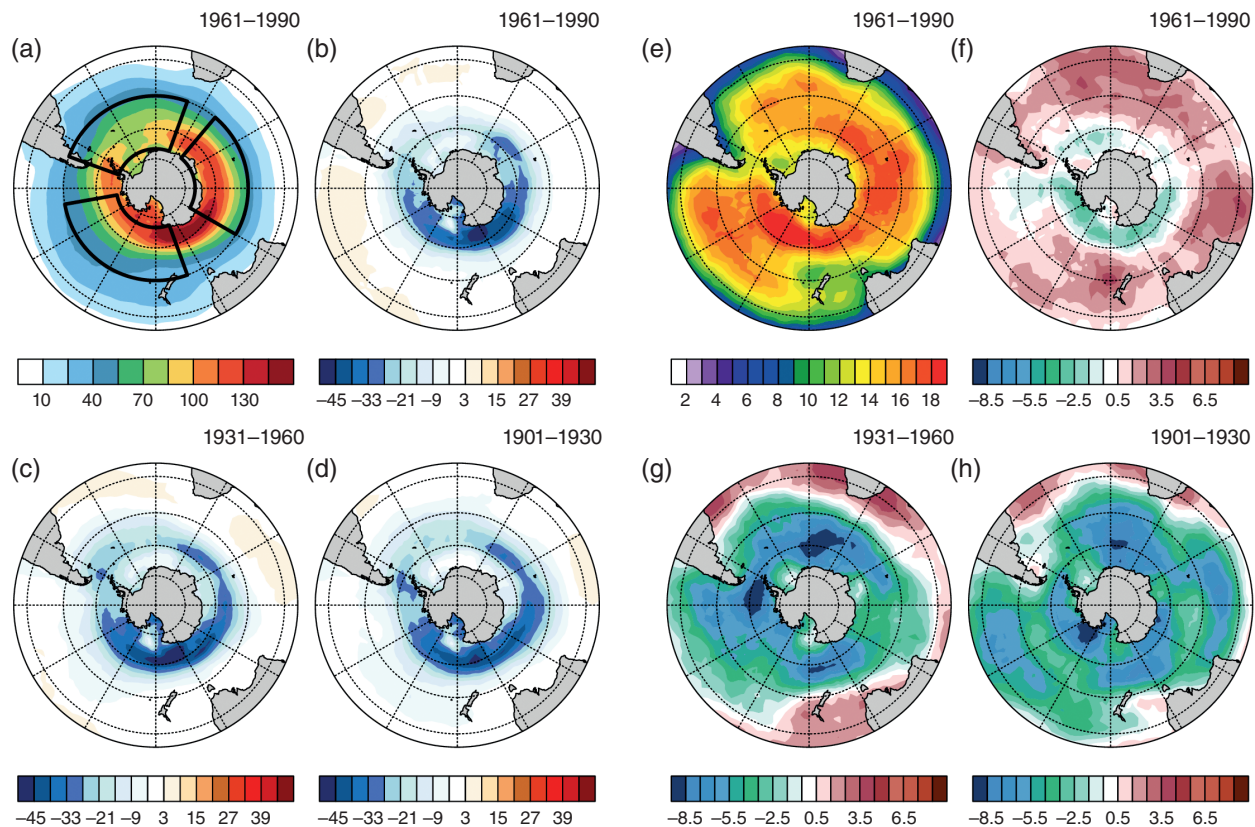
**Figure 4.** Track densities for cyclones (a−d) and windstorms (e−h) over the Southern Hemisphere in number of events per season. Cyclones: (a) ERA-20C (1961−1990), (b) NOAA-20CR minus ERA-20C (1961−1990), (c) NOAA-20CR minus ERA-20C (1931−1960) and (d) NOAA-20CR minus ERA-20C (1901−1930). Windstorms: (e) ERA-20C (1961−1990), (f) NOAA-20CR minus ERA-20C (1961−1990), (g) NOAA-20CR minus ERA-20C (1931−1960) and (h) NOAA-20CR minus ERA-20C (1901−1930). Southern Hemispheric regions used for time series analyses (Atlantic Ocean, Indian Ocean, Pacific Ocean) are shown in (a).

In general, HFV of both datasets is in better agreement for intense cyclones than those for all cyclones (except for very similar correlations of 0.87 and 0.83, respectively, during the third period over the North Atlantic).

### 3.1.3. Windstorm events

The two main centres of windstorm activity over the Pacific and Atlantic oceans (cf. e.g. Leckebusch *et al.*, 2008; Kruschke *et al.*, 2015) are well represented by ERA-20C during the period from 1961 until 1990 (Figure 1(e)). For this period differences between both datasets are comparatively small and partly related to the different height level used to identify windstorm events. As expected, absolute differences between both datasets decrease from the beginning to the end of the 20th century (Figure 1(f)−(h)). For the period from 1901 until 1930 (Figure 1(h)) more windstorm events in NOAA-20CR compared to ERA-20C are found mostly over the Polar Region in line with the enhanced cyclone activity for the same region and period in NOAA-20CR (Figure 1(d)).

Regional trends of windstorms are similar to extreme cyclone events (Figure 3). Large differences are found during the first and second period over the Northern Hemisphere/Polar Region, which is caused by the large number of windstorms in NOAA-20CR around 1920

(Figure 3(h)). In contrast, ERA-20C shows an increasing trend in windstorms during the 20th century in all regions. Similar to results obtained for cyclones, a good agreement with respect to the long-term trends is found for the last period.

The HFV of windstorms is in good agreement, with positive correlations for all periods and generally higher correlations for the last period. This is similar to the results obtained for all cyclone and extreme cyclone events.
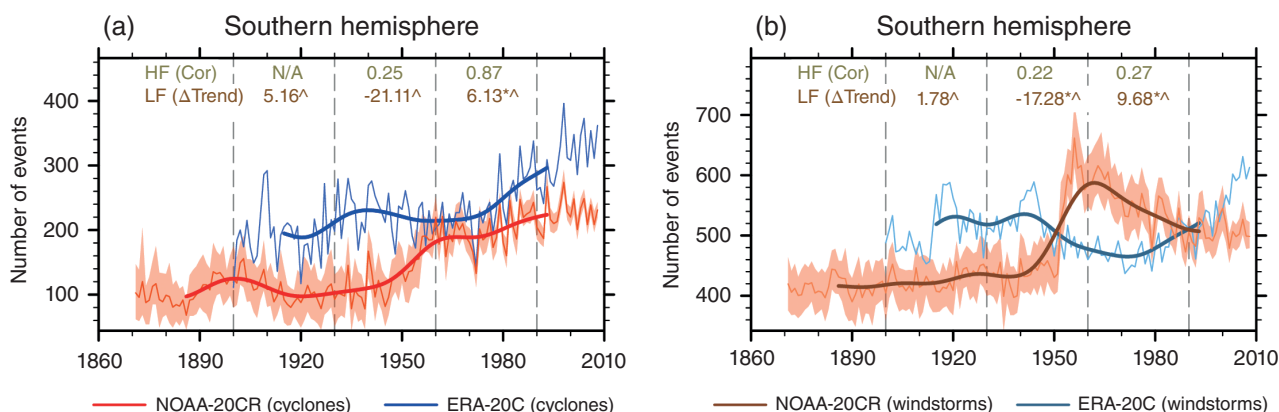
## 3.2. Southern Hemisphere (SH)

### 3.2.1. All cyclone events

More cyclones over most parts of the SH are found in ERA-20C compared to those in NOAA-20CR (Figure 4(b)−(d)), again related to differences in the horizontal resolution. The overall mean difference is about 12% (1961−1990), whereas there are on average around 10% fewer cyclones when interpolating ERA-20C to the coarser NOAA-20CR grid compared to the original ERA-20C data. These absolute differences tend to get smaller over time, with the highest deviations at the beginning of the 20th century (Figure 4(d)).

In NOAA-20CR, an increased cyclone activity around 1970 is found in all regions except the Pacific Ocean (Figure 2(e)−(h)), followed by a negative trend.

**Figure 5.** Time series of extreme cyclone events (minimum core pressure below 960 hPa) (a) and windstorm events (b) over the extra-tropical Southern Hemisphere. Time series, correlations and trend characteristics analogue to Figure 2.

In contrast, ERA-20C shows an increasing trend of cyclone events over the entire 20th century. LFV is in good agreement during the second period with long-term trends having the same sign. For the third period different signs of the regression coefficients in all regions except the Pacific Ocean are present, but most of these trends are not statistically significant. However, large deviations between both datasets regarding the magnitudes of relative trends at the end of the century are found, especially over the Atlantic Ocean (2.8% per decade) for which both time series are diverging at the end of the century.

Correlations coefficients of high-pass filtered time series are mostly positive, except for the Pacific during the second period. However, the agreement of both datasets is smaller compared to results carried out for the Northern Hemisphere.

### 3.2.2. Extreme cyclone events

For extreme cyclone events (core pressure below 960 hPa) a positive trend from 1920 until 2000 is present in NOAA-20CR (Figure 5(a)). ERA-20C shows a local maximum around 1940 and a local minimum at the beginning of the 20th century and around 1960. Best agreements regarding LFV is found for the first and third periods, whereas different signs of the regression coefficients are found for the second period with both linear trends being significantly different from zero.

Similarly, HFV shows highest agreement for the last period with a correlation coefficient of about 0.85, whereas it is only about 0.25 for the second period.

### 3.2.3. Windstorm events

The spatial distribution of windstorms in ERA-20C over the Southern Hemisphere for the period 1971–2000 indicates high windstorm activity over the Pacific and Indian Ocean and to a lesser extent over the Atlantic Ocean (Figure 4(e)). The largest differences are found for the first period (Figure 4(h)) characterized by a higher number of events in ERA-20C compared to those in NOAA-20CR. These differences decrease during the 20th century (Figure 4(g) and (h)).

Over the entire SH, NOAA-20CR shows a maximum of windstorms around 1960 (Figure 5(b)), similar to the results for all cyclones (Figure 2(e)). ERA-20C shows fewer events around 1970, followed by a positive trend until the end of the century. Trends show the same sign in the first period, but differ in the second and third period. Additionally, the magnitudes of the trends show high deviations of up to 17% per decade for the second period. HFV is in better agreement than LFV, with positive but small correlations for both periods of about 0.2.

## 4. Discussion and conclusion

In this study, cyclones and windstorms in the NOAA-20CR and ERA-20C 20th century reanalyses are analysed regarding their spatial distribution and temporal evolution over the Northern and Southern Hemispheres. Differences in long-term trends are assessed by comparing the linear regression coefficients derived from both datasets and three periods: 1901–1930, 1931–1960 and 1961–1990. The similarity of the HFV is obtained by calculating correlation coefficients between both high-passed filtered time series.

Substantial differences regarding the long-term trend of both, cyclones and windstorms between NOAA-20CR and ERA-20C are found over both hemispheres. This is partly expressed by different signs of the linear regression coefficients as well as by large differences regarding their magnitudes. Deviations tend to be largest for the beginning of the last century with better agreement for the second part of the 20th century in most cases.

Over the Northern Hemisphere, different signs of long-term trends are partly related to an enhanced cyclone and windstorm activity around 1920 followed by a decreasing trend of events in NOAA-20CR (also found by Wang *et al.*, 2013). In contrast, ERA-20C shows increasing numbers of cyclone/ windstorm events over the Polar Region between 1910 and 1960. For all cyclones, the magnitudes of the trends

differ drastically especially during the second period (1931–1960) over the Northern Hemisphere and Polar Region, but large deviations of the trend magnitudes over Northern Europe and the North Atlantic are also found at the end of the 20th century. The agreement of long-term trends is higher for extreme cyclones compared to all cyclones with the same sign in linear trends for both datasets in most periods. However, large differences regarding their magnitudes are present. Large deviations of long-term trends are also found for windstorm events over the NH, with largest differences around 1920, possibly related to the large differences in cyclone frequency during this time. Similar to extreme cyclones, both datasets show similar long-term trends in terms of their signs for windstorms over Northern Europe and the North Atlantic. In general, there is a better agreement of HFV compared to LFV with mostly positive correlations even if long-term trends differ substantially in sign and/or magnitude.

Over the Southern Hemisphere, different long-term trends for all cyclones, extreme cyclones and windstorms are also present. For all cyclones over the Atlantic Ocean differences are most striking at the end of the 20th century, where time series of track numbers diverge. Similarly to the NH, the agreement of HFV in both datasets is higher than for LFV with mostly positive correlations. However, results for the SH indicate less agreement for both LFV and HFV compared to the NH.

As pointed out by Wang *et al.* (2013) inhomogeneities in cyclone counts in NOAA-20CR are related to the changing number of observational counts during the 20th century and this might also be the case for ERA-20C. Differences might partly arise from the assimilation of near-surface winds over the oceans in ERA-20C, which was not done in NOAA-20CR. Furthermore, differences in the assimilation schemes themselves might lead to differences how observations are used to generate the respective reanalysis product, e.g. it is found that in most of the tropical cyclones bogus observations are rejected by ERA-20C (Poli *et al.*, 2015). Please refer to Poli and National Center for Atmospheric Research Staff (2016) for a brief overview about similarities and differences between ERA-20C and NOAA-20CR. A detailed analysis of the effects of these differences in generating the reanalysis datasets on windstorms and cyclones is beyond the scope of this paper, but might be crucial to understand discrepancies in long-term trends. Here, case studies for two storm events affecting the European continent during the early and late 20th century are analysed. Results suggest that there is less agreement between ERA-20C and NOAA-20CR for the storm in November 1928 with respect to its development (see Figure S1–S3; Supporting information) compared to storm *Kyrill* in January 2007 (see Figure S4–S6).

In summary, our results show that analyses of long-term trends of cyclone and windstorm events using both datasets should be interpreted carefully. In our opinion, it seems to be difficult to extend cyclone and windstorm event time series backwards to before around 1950 using NOAA-20CR and ERA-20C. However, as HFV is generally in better agreement than LFV, we conclude that investigations on shorter timescales can be useful if dataset-specific long-term trends are taken into account and properly removed.

## Acknowledgements

## Supporting information

The following supporting information is available:

**Appendix S1.** Case studies of two extreme storm situation within the 20th century.

**Figure S1.** Storm on 23/24. November 1928 as represented in NOAA-20CR (top panel) and ERA-20C (bottom panel). Mean sea level pressure (MSLP) fields given as filled contours and arrows indicate regions with wind speeds exceeding 15 m s$^{-1}$ (on the 0.995 sigma level for NOAA-20CR and 10-m height for ERA-20C). Furthermore, the ensemble standard deviation of MSLP is given for NOAA-20CR (grey lines).

**Figure S2.** Cyclone tracks for the event in November 1928 as represented in 28 selected NOAA-20CR members (blue lines) and ERA-20C (red line). Additionally, another cyclone track over the Mediterranean region is included.

**Figure S3.** Windstorm tracks for the event in November 1928 as represented in 28 selected NOAA-20CR members (blue lines) and ERA-20C (red line).

**Figure S4.** Storm Kyrill on 17/19. January 2007 as represented in NOAA-20CR (top panel) and ERA-20C (bottom panel). Mean sea level pressure (MSLP) fields given as filled contours and arrows indicate regions with wind speeds exceeding 15 m s$^{-1}$ (on the 0.995 sigma level for NOAA-20CR and 10-m height for ERA-20C). Furthermore, the ensemble standard deviation of MSLP is given for NOAA-20CR (grey lines).

**Figure S5.** Cyclone tracks for storm Kyrill as represented in 28 selected NOAA-20CR members (blue lines) and ERA-20C (red line).

**Figure S6.** Windstorm tracks for storm Kyrill as represented in 28 selected NOAA-20CR members (blue lines) and ERA-20C (red line).

## References

Befort DJ, Fischer M, Leckebusch GC, Ulbrich U, Ganske A, Rosenhagen G, Heinrich H. 2015. Identification of storm surge events over the German Bight from atmospheric reanalysis and climate model data. *Natural Hazards and Earth System Sciences* **15**(6): 1437–1447.

Brönnimann S, Martius O, von Waldow H, Welker C, Luterbacher J, Compo GP, Sardeshmukh PD, Usbeck T. 2012. Extreme winds at northern mid-latitudes since 1871. *Meteorologische Zeitschrift* **21**(1): 13–27.

Compo GP, Whitaker JS, Sardeshmukh PD, Matsui N, Allan RJ, Yin X, Gleason BE, Vose RS, Rutledge G, Bessemoulin P, Brönnimann S, Brunet M, Crouthamel RI, Grant AN, Groisman PY, Jones PD, Kruk MC, Kruger AC, Marshall GJ, Maugeri M, Mok HY, Nordli Ø, Ross TF, Trigo RM, Wang XL, Woodruff SD, Worley SJ. 2011. The twentieth century reanalysis project. *Quarterly Journal of Royal Meteorological Society* **137**(654): 1–28, doi: 10.1002/qj.776.

Donat MG, Renggli D, Wild S, Alexander LV, Leckebusch GC, Ulbrich U. 2011. Reanalysis suggests long-term upward trends in European storminess since 1871. *Geophysical Research Letters* **38**: L14703, doi: 10.1029/2011GL047995.

Duchon CE. 1979. Lanczos filtering in one and two dimensions. *Journal of Applied Meteorology* **18**(8): 1016–1022, doi: 10.1175/1520-0450(1979)018<1016:LFIOAT>2.0.CO;2.

Hewson TD, Neu U. 2015. Cyclones, windstorms and the IMILAST project. *Tellus A* **67**: 27128, doi: 10.3402/tellusa.v67.27128.

Huntingford C, Marsh T, Scaife AA, Kendon EJ, Hannaford J, Kay AL, Lockwood M, Prudhomme C, Reynard NS, Parry S, Lowe JA, Screen JA, Ward HC, Roberts M, Stott PA, Bell VA, Bailey M, Jenkins A, Legg T, Otto FEL, Massey N, Schaller N, Slingo J, Allen MR. 2014. Potential influences on the United Kingdom's floods of winter 2013/14. *Nature Climate Change* **4**(9): 769–777, doi: 10.1038/nclimate2314.

Kendon M, McCarthy M. 2015. The UK's wet and stormy winter of 2013/2014. *Weather* **70**(2): 40–47, doi: 10.1002/wea.2465.

Krueger O, Schenk F, Feser F, Weisse R. 2013. Inconsistencies between long-term trends in storminess derived from the 20CR reanalysis and observations. *Journal of Climate* **26**(3): 868–874, doi: 10.1175/JCLI-D-12-00309.1.

Krueger O, Feser F, Bärring L, Kaas E, Schmith T, Tuomenvirta H, von Storch H. 2014. Comment on "Trends and low frequency variability of extra-tropical cyclone activity in the ensemble of twentieth century reanalysis" by Xiaolan L. Wang, Y. Feng, G. P. Compo, V. R. Swail, F. W. Zwiers, R. J. Allan, and P. D. Sardeshmukh, Climate Dynamics, 2012. *Climate Dynamics* **42**(3): 1127–1128, doi: 10.1007/s00382-013-1814-9.

Kruschke T. 2015. Winter wind storms: Identification, verification of decadal predictions, and regionalization. PhD thesis, Department of Earth Sciences, Institute of Meteorology, Freie Universität Berlin, Berlin, Germany. http://www.diss.fu-berlin.de/diss/receive/FUDISS_thesis_000000099397 (accessed 15 February 2016).

Kruschke T, Rust HW, Kadow C, Leckebusch GC, Ulbrich U. 2014. Evaluating decadal predictions of northern hemispheric cyclone frequencies. *Tellus A* **66**: 22830.

Kruschke T, Rust HW, Kadow C, Müller WA, Pohlmann H, Leckebusch GC, Ulbrich U. 2015. Probabilistic evaluation of decadal prediction skill regarding Northern Hemisphere winter storms. *Meteorologische Zeitschrift* (early online release) doi: 10.1127/metz/2015/0641.

Lambert SJ, Fyfe JC. 2006. Changes in winter cyclone frequencies and strengths simulated in enhanced greenhouse warming experiments: results from the models participating in the IPCC diagnostic exercise. *Climate Dynamics* **26**(7): 713–728, doi: 10.1007/s00382-006-0110-3.

Leckebusch GC, Ulbrich U. 2004. On the relationship between cyclones and extreme windstorm events over Europe under climate change. *Global and Planetary Change* **44**(1–4): 181–193.

Leckebusch GC, Koffi B, Ulbrich U, Pinto JG, Spangehl T, Zacharias S. 2006. Analysis of frequency and intensity of European winter storm events from a multi-model perspective, at synoptic and regional scales. *Climate Research* **31**: 59–74.

Leckebusch GC, Renggli D, Ulbrich U. 2008. Development and application of an objective storm severity measure for the Northeast Atlantic region. *Meteorologische Zeitschrift* **17**(5): 575–587, doi: 10.1127/0941-2948/2008/0323.

Lim E-P, Simmonds I. 2002. Explosive cyclone development in the Southern Hemisphere and a comparison with Northern Hemisphere events. *Monthly Weather Review* **130**(9): 2188–2209, doi: 10.1175/1520-0493(2002)130<2188:ECDITS>2.0.CO;2.

Matthews T, Murphy C, Wilby RL, Harrigan S. 2014. Stormiest winter on record for Ireland and UK. *Nature Climate Change* **4**(9): 738–740, doi: 10.1038/nclimate2336.

Murray RJ, Simmonds I. 1991. A numerical scheme for tracking cyclone centres from digital data. Part I: development and operation of the scheme. *Australian Meteorological Magazine* **39**(3): 155–166.

Neu U, Akperov MG, Bellenbaum N, Benestad R, Blender R, Caballero R, Cocozza A, Dacre HF, Feng Y, Fraedrich K, Grieger J, Gulev S, Hanley J, Hewson T, Inatsu M, Keay K, Kew SF, Kindem I, Leckebusch GC, Liberato MLR, Lionello P, Mokhov II, Pinto JG, Raible CC, Reale M, Rudeva I, Schuster M, Simmonds I, Sinclair M, Sprenger M, Tilinina ND, Trigo IF, Ulbrich S, Ulbrich U, Wang XL, Wernli H. 2013. IMILAST: a community effort to intercompare extratropical cyclone detection and tracking algorithms. *Bulletin of the American Meteorological Society* **94**(4): 529–547, doi: 10.1175/BAMS-D-11-00154.1.

Nissen KM, Ulbrich U, Leckebusch GC, Kuhnel I. 2014a. Decadal windstorm activity in the North Atlantic-European sector and its relationship to the meridional overturning circulation in an ensemble of simulations with a coupled climate model. *Climate Dynamics* **43**(5): 1545–1555, doi: 10.1007/s00382-013-1975-6.

Nissen KM, Leckebusch GC, Pinto JG, Ulbrich U. 2014b. Mediterranean cyclones and windstorms in a changing climate. *Regional Environmental Change* **14**(5): 1873–1890, doi: 10.1007/s10113-012-0400-8.

Pinto JG, Spangehl T, Ulbrich U, Speth P. 2005. Sensitivities of a cyclone detection and tracking algorithm: individual tracks and climatology. *Meteorologische Zeitschrift* **14**(6): 823–838.

Poli P, National Center for Atmospheric Research Staff (Eds). 2016. The climate data guide: ERA-20C: ECMWF's atmospheric reanalysis of the 20th century (and comparisons with NOAA's 20CR). https://climatedataguide.ucar.edu/climate-data/era-20c-ecmwfs-atmospheric-reanalysis-20th-century-and-comparisons-noaas-20cr. See more at: https://climatedataguide.ucar.edu/climate-data/era-20c-ecmwfs-atmospheric-reanalysis-20th-century-and-comparisons-noaas-20cr#sthash.Nchqcn9o.dpuf (accessed 15 February 2016).

Poli P, Hersbach H, Tan D, Dee D, Thépaut J-N, Simmons A, Peubey C, Laloyaux P, Komori T, Berrisford P, Dragani R, Trémolet Y, Hólm E, Bonavita M, Isaksen L, Fisher M. 2013. The data assimilation system and initial performance evaluation of the ECMWF pilot reanalysis of the 20th-century assimilating surface observations only (ERA-20C). ERA Report Series 14, European Centre for Medium-Range Weather Forecasts, Reading, UK.

Poli P, Hersbach H, Berrisford P, Dee D, Simmons A, Laloyaux P. 2015. ERA-20C deterministic. ERA Report Series 20, European Centre for Medium-Range Weather Forecasts, Reading, UK.

Rayner NA, Parker DE, Horton EB, Folland CK, Alexander LV, Rowell DP, Kent EC, Kaplan A. 2003. Global analyses of sea surface temperature, sea ice, and night marine air temperature since the late nineteenth century. *Journal of Geophysical Research* **108**(D14): 4407, doi: 10.1029/2002JD002670.

Renggli D, Leckebusch GC, Ulbrich U, Gleixner SN, Faust E. 2011. The skill of seasonal ensemble prediction systems to forecast wintertime windstorm frequency over the North Atlantic and Europe. *Monthly Weather Review* **139**(9): 3052–3068, doi: 10.1175/2011MWR3518.1.

Revell CG. 2015. A note on a Southern Ocean storm. *Weather* **70**(1): 25–26, doi: 10.1002/wea.2337.

Titchner HA, Rayner NA. 2014. The Met Office Hadley Centre sea ice and sea-surface temperature data set, version 2: 1. Sea ice concentrations. *Journal of Geophysical Research* **119**: 2864–2889, doi: 10.1002/2013JD020316.

Ulbrich U, Leckebusch GC, Grieger J, Schuster M, Akperov M, Bardin MY, Feng Y, Gulev S, Inatsu M, Keay K, Kew SF, Liberato ML, Lionello P, Mokhov II, Neu U, Pinto JG, Raible CC, Reale M, Rudeva I, Simmonds I, Tilinina ND, Trigo IF, Ulbrich S, Wang XL, Wernli H, Team IMILAST. 2013. Are greenhouse gas signals of Northern Hemisphere winter extra-tropical cyclone activity dependent on the

identification and tracking algorithm? *Meteorologische Zeitschrift* **22**(1): 61–68, doi: 10.1127/0941-2948/2013/0420.

Wang XL, Feng Y, Compo GP, Swail VR, Zwiers FW, Allan RJ, Sardeshmukh PD. 2013. Trends and low frequency variability of extra-tropical cyclone activity in the ensemble of twentieth century reanalysis. *Climate Dynamics* **40**(11): 2775–2800, doi: 10.1007/s00382-012-1450-9.

Wang XL, Feng Y, Compo GP, Zwiers FW, Allan RJ, Swail VR, Sardeshmukh PD. 2014. Is the storminess in the twentieth century reanalysis really inconsistent with observations? A reply to the comment by Krueger et al. (2013b). *Climate Dynamics* **42**(3): 1113–1125, doi: 10.1007/s00382-013-1828-3.

Wild S, Befort DJ, Leckebusch GC. 2015. Was the extreme storm season 2013–14 over the North Atlantic and the United Kingdom triggered by changes in the West-Pacific Warm Pool? *Bulletin of the American Meteorological Society* **96**(12): S29–S34, doi: 10.1175/BAMS-EEE_2014_ch7.1.

Yu L, Weller RA. 2007. Objectively analyzed air–sea heat fluxes for the global ice-free oceans (1981–2005). *Bulletin of the American Meteorological Society* **88**: 527–539.